

Collaborative Indirect Influencing and Control on Graphs using Graph Neural Networks

Max L. Gardenswartz, Brandon C. Fallin, Cristian F. Nino, and Warren E. Dixon

Abstract—This paper presents a novel approach to solving the indirect influence problem in networked systems, in which cooperative nodes must regulate a target node with uncertain dynamics to follow a desired trajectory. We leverage the message-passing structure of a graph neural network (GNN), allowing nodes to collectively learn the unknown target dynamics in real time. We develop a novel GNN-based backstepping control strategy with formal stability guarantees derived from a Lyapunov-based analysis. Numerical simulations are included to demonstrate the performance of the developed controller.

Index Terms—Nonlinear systems, adaptive control, neural networks

I. INTRODUCTION

Networks of interconnected agents operate across a variety of domains including social media, financial markets, traffic systems, and crowd management. The flow of information and actions in these networks is formalized through graph theory, where individual actors are represented as nodes and connections as edges. This representation of a system enables analysis of how individual nodes' actions propagate through the network. In scenarios like guiding wildlife populations or regulating opinion dynamics in virtual networks, individual nodes must leverage inter-agent interactions to accomplish network-wide goals [1], [2]. We refer to these scenarios as the indirect influence problem.

Various methodologies have been employed to address the indirect influence problem. Model-based implicit control strategies have enabled coordinated influence of uncooperative targets with heterogeneous nonlinear dynamics [3] and *switched* systems analysis has facilitated the development of indirect influence strategies based on system characteristics of each uncooperative target [4]. Additionally, containment control strategies have permitted influencing agents to guide follower agents away from obstacles [5].

Existing approaches to the indirect influence problem face a variety of limitations. Model-based strategies struggle to

meet control objectives with uncertain or unstructured dynamics. Methods relying on individual leaders face scalability challenges when confronted with numerous targets, or when targets exhibit high mobility relative to the leaders. Further, when influence must be coordinated across multiple actors to regulate a target's state, individual learning fails to capitalize on shared knowledge. Based on these drawbacks, learning-based methods with distributed information sharing are motivated for addressing the indirect influence problem.

Neural networks are powerful tools for approximating continuous functions over compact domains [6], [7], [8]. Recent work has extended Lyapunov-based adaptive control methods from shallow neural networks to DNNs, which have been shown to provide improved function approximation performance with fewer parameters [9], [10], [11]. Notably, in [12], a single leader agent uses a Lyapunov-based DNN (Lb-DNN) to learn unknown inter-agent interaction dynamics in real time, allowing for the leader to regulate each uncontrolled agent to within a ball of the desired state. This approach has been extended to address target tracking with partial state feedback, enabling agents to reconstruct target states from limited measurements while simultaneously learning unknown target dynamics, and distributed adaptation approaches have further enhanced these methods by enabling coordinated learning across multiple agents [13]. Lb-DNNs have also been leveraged with approximate dynamic programming to explore optimal online solutions to the indirect influencing problem [14], [15].

Graph neural networks (GNNs) have emerged as a powerful tool for distributed control applications due to their message-passing framework, which naturally facilitates information exchange between networked agents. This framework provides specific advantages for addressing the indirect influence problem by encoding the network structure directly into the neural network architecture. Previously, GNNs have been used to perform autonomous path planning in multi-robot systems [16] and develop decentralized controllers for multi-agent flocking [17]. When applied to multi-agent control, GNNs are typically trained offline and subsequently deployed in a decentralized, open-loop manner [18], [19]. However, the data sets against which these networks are trained may not sufficiently represent all operating conditions, and the resulting systems may be unable to adapt online to disturbances. The combination of GNNs with Lyapunov-based update laws (i.e., Lb-GNNs) addresses these shortcomings, enabling real-time

Max L. Gardenswartz, Brandon C. Fallin, Cristian F. Nino, and Warren E. Dixon are with the Department of Mechanical and Aerospace Engineering, University of Florida, Gainesville, FL 32611, USA. Email: {mgardenswartz, brandonfallin, cristian1928, wdixon}@ufl.edu.

This research is supported in part by AFOSR grant FA8651-24-1-0018. Any opinions, findings, and conclusions or recommendations expressed in this material are those of the author(s) and do not necessarily reflect the views of the sponsoring agency.

adaptation for distributed control tasks [20].

This work addresses an indirect influence problem using a deep Lb-GNN-based backstepping controller to approximate unknown inter-agent interaction dynamics. We formulate the problem with a team of cooperative nodes seeking to influence a target node and regulate it to follow a desired trajectory. We leverage the deep Lb-GNN's inherent ability to share learned information, allowing the team of cooperative nodes to collectively approximate the unknown target dynamics in a distributed manner. Our method achieves online learning without prior data collection, making it adaptable to changing system conditions. Our approach scales effectively with network size by distributing the influence workload across multiple influencing agents. The analytic results are empirically validated with a numerical simulation.

II. PRELIMINARIES

A. Notation

Let \mathbb{R} and \mathbb{Z} denote the sets of reals and integers, respectively. For $x \in \mathbb{R}$, let $\mathbb{R}_{\geq x} \triangleq [x, \infty)$ and $\mathbb{Z}_{\geq x} \triangleq \mathbb{R}_{\geq x} \cap \mathbb{Z}$. Let \mathbf{h}_i represent the i^{th} standard basis in \mathbb{R}^N , where the standard basis is made up of vectors that have one entry equal to 1 and the remaining $N - 1$ entries equal to 0. The $p \times p$ identity matrix and the $p \times 1$ column vector of ones are denoted by I_p and $\mathbf{1}_p$, respectively. The $m \times n$ column vector of zeros is denoted by $\mathbf{0}_{m \times n}$. The enumeration operator $[\cdot]$ is defined as $[N] \triangleq \{1, 2, \dots, N\}$. Given a positive integer N and collection $\{x_i\}_{i \in [N]}$, let $[x_i]_{i \in [N]} \triangleq [x_1, x_2, \dots, x_N] \in \mathbb{R}^{m \times N}$ for $x_i \in \mathbb{R}^m$. The cardinality of a set A is denoted by $|A|$. For a set A and an input x , the indicator function is denoted by $\mathbb{1}_A(x)$, where $\mathbb{1}_A(x) = 1$ if $x \in A$, and $\mathbb{1}_A(x) = 0$ otherwise. For $x \in \mathbb{R}^m$, let $\text{diag}\{\cdot\}$ denote the diagonalization operator which assigns the i^{th} value of x to the i^{th} entry of an output $m \times m$ matrix for all $i \in [m]$. Similarly, let $\text{blkdiag}\{\cdot\}$ denote the block diagonalization operator. For $A \in \mathbb{R}^{m \times n}$ and $B \in \mathbb{R}^{p \times q}$,

$$\text{blkdiag}\{A, B\} \triangleq \begin{bmatrix} A & \mathbf{0}_{m \times q} \\ \mathbf{0}_{p \times n} & B \end{bmatrix},$$

where $\mathbf{0}_{m \times q} \in \mathbb{R}^{m \times q}$ is the $m \times q$ matrix of zeros and $\text{blkdiag}\{A, B\} \in \mathbb{R}^{(m+p) \times (n+q)}$. Given $A \in \mathbb{R}^{m \times n}$ with columns $[a_i]_{i \in [n]}^T \subset \mathbb{R}^m$, $\text{vec}(A) \triangleq [a_1^T, a_2^T, \dots, a_n^T]^T \in \mathbb{R}^{mn}$.

B. Graphs

For $N \in \mathbb{Z}_{>0}$, let $G \triangleq (V, E)$ be a static and undirected graph with node set $V \triangleq [N]$ and edge set $E \subseteq V \times V$. The edge $(i, j) \in E$ if and only if the node i can send information to node j . In this work, G is undirected, so $(i, j) \in E$ if and only if $(j, i) \in E$. Let $A \triangleq [a_{ij}] \in \mathbb{R}^{N \times N}$ denote the adjacency matrix of G , where $a_{ij} = \mathbb{1}_E(i, j)$ and $a_{ii} = 0$ for all $i \in V$. An undirected graph is connected if and only if there exists a sequence of edges in E between any two nodes in V . The neighborhood of node i is denoted by \mathcal{N}_i , where $\mathcal{N}_i \triangleq \{j \in V : (j, i) \in E\}$. The augmented neighborhood of node i is denoted by $\bar{\mathcal{N}}_i$, where $\bar{\mathcal{N}}_i \triangleq \mathcal{N}_i \cup \{i\}$. The set of node i 's k -hop neighbors is denoted by \mathcal{N}_i^k . The degree matrix of G is denoted by $D \triangleq \text{diag}(A\mathbf{1}_N)$. The Laplacian

matrix of G is denoted by $\mathcal{L}_G \triangleq D - A \in \mathbb{R}^{N \times N}$. In this work, we focus on a class of communication networks where information flows through all nodes, which occurs when the graph G is connected.

The set of permutations on $[N]$ is denoted by S_N . For a graph G and a permutation S_N , we define the graph permutation operation as $p * G$, where $p \in S_N$. Formally, two graphs G_1 and G_2 are isomorphic if they have the same number of nodes and there exists a permutation such that $G_1 = p * G_2$ [21].

C. Graph Neural Networks

The GNN architecture employs a message-passing framework in which nodes exchange and update vector-valued messages using feedforward layers. These messages are the outputs of each GNN layer calculated at the node level. The GNN processes an input graph G with a set of node features to generate node embeddings, which are the outputs of the final GNN layer at each node. In this framework, each node's output in a layer is informed by its previous layer output and messages received from neighboring nodes. We use superscripts to denote layer-specific elements. For example, $W_i^{(k)}$ denotes the i^{th} node's weights for the k^{th} GNN layer. Subscripts indicate the specific node where an embedding or function is applied.

Let the activation function for the k^{th} GNN layer at node i be denoted by $\sigma^{(k)}(\cdot)$, where $\sigma(\cdot)$ is an element-wise, smooth, bounded nonlinearity with bounded first and second derivatives appended with 1 to allow for biases such that for $x \in \mathbb{R}^m$, $\sigma(x) = [\sigma(x_0), \dots, \sigma(x_m), 1]^T$. Let the output of layer j for node i of the GNN be denoted by $\phi_i^{(j)}$. Let the aggregation function for the GNN at node i be denoted by $\sum_{m \in \bar{\mathcal{N}}_i} \phi_m^{(k-1)}$. Additionally, let $d^{(j)}$ represent the number of features at the j^{th} layer of the GNN for $j = 0, \dots, k$, where j denotes the layer index. Let $d^{(in)}$ denote the dimension of the GNN input at the base layer of each node. Let $d^{(out)}$ denote the output dimension of the output layer of each node. Let $d^{(j)} = d^{(in)} + 1$ when $j = -1$ and $d^{(j)} = d^{(out)}$ when $j = k$.

Next, we define the deep GNN architecture for an arbitrary number of layers. Let $\bar{\kappa}_i$ denote the i^{th} node's input augmented with a bias term such that $\bar{\kappa}_i \triangleq [\kappa_i^T, 1]^T \in \mathbb{R}^{d^{(in)}+1}$. Let $\bar{\kappa} \triangleq [\bar{\kappa}_1, \dots, \bar{\kappa}_N] = [\bar{\kappa}_i]_{i \in V} \in \mathbb{R}^{(d^{(in)}+1) \times N}$. To distinguish between node indices in cascading layers, we let $m^{(j)}$ denote an arbitrary index corresponding to the j^{th} layer, where $m^{(j)} \in V$. Then, we let $\mathbf{m}^{(j)}$ denote $m^{(j)} \in V$. Let $\phi^{(j)} \triangleq [\phi_1^{(j)}, \dots, \phi_N^{(j)}] = [\phi_i^{(j)}]_{m^{(j)}} \in \mathbb{R}^{(d^{(j-1)}+1) \times N}$. Let $\bar{A} \in \mathbb{R}^{N \times N}$ represent the adjacency matrix with self loops, and $\bar{A}_i \in \mathbb{R}^{1 \times N}$ represent the i^{th} row of the adjacency matrix. The GNN architecture at node i is expressed as

$$\phi_i^{(j)} \triangleq \begin{cases} \sigma^{(j)} \left(W_i^{(j)T} \bar{\kappa}_i^T \right), & j = 0, \\ \sigma^{(j)} \left(W_i^{(j)T} \phi^{(j-1)} \bar{A}_i^T \right), & j = 1, \dots, k-1, \\ W_i^{(j)T} \phi_i^{(j-1)}, & j = k, \end{cases} \quad (1)$$

for all $i \in V$, an input $y^{(j)} \in \mathbb{R}^m$, the partial derivative $\frac{\partial \sigma^{(j)}}{\partial y^{(j)}} : \mathbb{R}^{d^{(j)}} \rightarrow \mathbb{R}^{(d^{(j)}+1) \times d^{(j)}}$ of the activation function vector at the j^{th} layer with respect to its input is given as $[\sigma'^{(j)}(y_1)\mathbf{h}_1, \dots, \sigma'^{(j)}(y_{d^{(j)}})\mathbf{h}_{d^{(j)}}, \mathbf{0}_{d^{(j)}}]^T \in \mathbb{R}^{(d^{(j)}+1) \times d^{(j)}}$,

where \mathbf{h}_i is the i^{th} standard basis in $\mathbb{R}^{d^{(j)}}$ and $\mathbf{0}_{d^{(j)}}$ is the zero vector in $\mathbb{R}^{d^{(j)}}$. The vector of weights for the GNN at node i is defined as $\theta_i \in \mathbb{R}^{p_{\text{GNN}}}$, where

$$\theta_i \triangleq \left[\text{vec} \left(W_i^{(0)} \right)^\top, \dots, \text{vec} \left(W_i^{(k)} \right)^\top \right]^\top, \quad (2)$$

and $p_{\text{GNN}} \triangleq \sum_{j=0}^k (d^{(j)})(d^{(j-1)} + 1)$. For each node $i \in V$, the first partial derivative of the deep GNN architecture at node i in (1) with respect to (2) is

$$\frac{\partial \phi_i}{\partial \theta_i} \triangleq \left[\frac{\partial \phi_i}{\partial \text{vec} \left(W_i^{(0)} \right)}, \dots, \frac{\partial \phi_i}{\partial \text{vec} \left(W_i^{(k)} \right)} \right],$$

where $\frac{\partial \phi_i}{\partial \theta_i} \in \mathbb{R}^{d^{(\text{out})} \times p_{\text{GNN}}}$ [20, Lemma 1]. The closed form of the partial derivatives of ϕ_i with respect to $\text{vec}(W_i^{(\ell)})$ for all $\ell = 0, \dots, k$ is defined in [20, Table 1].

Let \mathcal{G}_N denote the set of undirected graphs with N nodes. Let $F \in \mathbb{R}^{N^m}$ denote the ensemble feature vector of the graph, where each node has features in \mathbb{R}^m . A function $f : \mathcal{G}_N \times \mathbb{R}^{N^m} \rightarrow \mathbb{R}^{N^\ell}$ on a graph G is called equivariant if $f(p * G, p * F) = p * f(G, F)$ for every permutation $p \in S_N$, every $G \in \mathcal{G}_N$, and every $F \in \mathbb{R}^{N^m}$ [21]. An example of an equivariant function on a graph is a continuous function of a node's features evaluated at that node. In this work, we approximate equivariant functions of the graph using a deep Lb-GNN.

The expressive power of deep GNNs is intrinsically linked to the message-passing framework [22]. This expressive ability can be formalized through the 1-Weisfeiler-Leman (1-WL) test, a graph isomorphism heuristic that iteratively refines node labels based on neighborhood information. The 1-WL test's ability to distinguish graph structures has been shown to be representative of the discriminative ability of the GNN architecture. The message-passing GNN in (1) universally approximates equivariant, graph-valued functions that are less separating the 2-WL test [21].

III. PROBLEM FORMULATION

In this section, we consider a network of N nodes tasked with collaboratively influencing a target node to follow a desired trajectory. The target node has unknown, unstructured interaction dynamics with respect to each influencing node and unknown, unstructured drift dynamics. The influencing nodes have homogeneous unknown, unstructured dynamics. The deep Lb-GNN architecture is used to learn the target node's unknown drift dynamics, the target node's unknown interaction dynamics, and the unknown interaction dynamics between influencing nodes.

A. Systems Dynamics

Consider a network of N influencing nodes indexed by $i \in V$ with the static, undirected communication graph $G = (V, E)$, where $N \geq 2$. The influencing nodes' objective is to collaboratively regulate the state of a target node to follow a desired trajectory. All influencing nodes can measure their relative states with respect to the target node. The state of the i^{th} influencing node is denoted by $y_i \in \mathbb{R}^n$, for all $i \in V$. Let $Q_i \triangleq$

$[(y_m \cdot \mathbf{1}_{\mathcal{N}_i}(m))^\top]_{m \in V}^\top \in \mathbb{R}^{nN}$ denote the concatenated states of the i^{th} influencing node and its neighbors. The dynamics of the i^{th} influencing node are

$$\dot{y}_i = f(Q_i) + u_i, \quad (3)$$

where $u_i \in \mathbb{R}^n$ denotes the i^{th} influencing node's control input and $f : \mathbb{R}^{nN} \rightarrow \mathbb{R}^n$ is an unknown, unstructured function that denotes the interaction dynamics between node i and its neighboring nodes, indexed by $j \in \mathcal{N}_i$. The target node is indirectly influenced by an unknown interaction function denoted by $g : \mathbb{R}^n \times \mathbb{R}^n \rightarrow \mathbb{R}^n$, which depends on the target node's state and an individual influencing node's state. Let the target node's state be denoted by $x_0 \in \mathbb{R}^n$. The dynamics of the target node are given as

$$\dot{x}_0 = h(x_0) + \sum_{i \in V} g(x_0, y_i)(x_0 - y_i), \quad (4)$$

where $h : \mathbb{R}^n \rightarrow \mathbb{R}^n$ is an unknown, unstructured function that denotes the target node's drift dynamics. The functions f , g , and h are assumed to be continuous. In practice, the target node's dynamics are often constrained by initial conditions and environmental factors which limit its state variations. This is formalized in the following assumption.

Assumption 3.1: [23, Assumption 1] There exist known constants $\bar{g} \in \mathbb{R}_{>0}$ and $\bar{h} \in \mathbb{R}_{>0}$ such that $\|g(x_0, y_i)\| \leq \bar{g}$ and $\|h(x_0)\| \leq \bar{h}$.

B. Control Objective

The influencing nodes' control objective is to regulate x_0 to a user-defined desired trajectory $x_d \in \mathbb{R}^n$ of class \mathcal{C}^1 , despite the target node's uncertain drift and interaction dynamics described by (4). To this end, we define the state tracking error $e \in \mathbb{R}^n$ as

$$e \triangleq x_0 - x_d. \quad (5)$$

Assumption 3.2: [13, Assumption 1] There exist known constants $\bar{x}_d \in \mathbb{R}$ and $\bar{\dot{x}}_d \in \mathbb{R}$ such that $\|x_d(t)\| \leq \bar{x}_d$ and $\|\dot{x}_d(t)\| \leq \bar{\dot{x}}_d$ for all $t \in [t_0, \infty)$.

Since the target node's dynamics in (4) do not explicitly contain a control input, a backstepping control technique is employed. The signal y_i is treated as a virtual control input. We define a backstepping error $\eta_i \in \mathbb{R}^n$ for the i^{th} influencing node as

$$\eta_i \triangleq y_{d,i} - y_i, \quad (6)$$

where $y_{d,i} \in \mathbb{R}^n$ denotes the i^{th} influencing node's desired trajectory for all $i \in V$. Substituting (4) into the time derivative of (5) and using (6) yields

$$\dot{e} = h(x_0) - \dot{x}_d + \sum_{i \in V} g(x_0, y_i)(x_0 + \eta_i - y_{d,i}). \quad (7)$$

IV. CONTROL SYNTHESIS

Based on the subsequent stability analysis, the desired trajectory of the i^{th} influencing node is designed as

$$y_{d,i} = k_1 e + x_d, \quad (8)$$

for all $i \in V$, where $k_1 \in \mathbb{R}_{>0}$ is a user-defined gain. Substituting (8) into (7) yields

$$\dot{e} = h(x_0) - \dot{x}_d + \sum_{i \in V} g(x_0, y_i) (\eta_i + (1 - k_1) e). \quad (9)$$

Substituting (3), (9), and the time derivative of (8) into the time derivative of (6) yields

$$\begin{aligned} \dot{\eta}_i &= k_1 \sum_{j \in V \setminus \mathcal{N}_i} g(x_0, y_j) (\eta_j + (1 - k_1) e) \\ &\quad + (1 - k_1) \dot{x}_d - u_i + F(R_i), \end{aligned} \quad (10)$$

where $F(R_i) \triangleq k_1 h(x_0) - f(Q_i) + \sum_{j \in \mathcal{N}_i} k_1 g(x_0, y_j) (\eta_j + (1 - k_1) e)$, $R_i \triangleq [x_0^\top, Q_i^\top]^\top \in \mathbb{R}^{d^{(in)}}$ for all $i \in V$, and $d^{(in)} = n(N + 1)$.

A. Function Approximation Capabilities of GNNs

To approximate the unknown inter-agent dynamics, we leverage the universal function approximation properties of GNNs established in [21]. To this end, we define the deep Lb-GNN $\Phi \triangleq [\phi_i^\top]_{i \in V}^\top$, with p total weights at each node i . The output of a k -layer Lb-GNN Φ at node i is a function of its $(k - 1)$ -hop neighbor's weights, $(\theta_j)_{j \in \mathcal{N}_i^{k-1}}$, and its k -hop neighbor's inputs, $(R_j)_{j \in \mathcal{N}_i^k}$. Node i 's component of the Lb-GNN Φ is denoted by $\phi_i \triangleq \phi_i(R_i, (R_j)_{j \in \mathcal{N}_i^k}, \theta_i, (\theta_j)_{j \in \mathcal{N}_i^{k-1}})$. Let the input to the Lb-GNN Φ be denoted as $R \triangleq [R_i^\top]_{i \in V}^\top \in \mathcal{Y}$, where $\mathcal{Y} \subset \mathbb{R}^{Nd^{(in)}}$. Let Ω denote the compact set over which the universal function approximation property of GNNs holds. We use the Lb-GNN Φ to approximate the function $H : \mathbb{R}^{Nd^{(in)}} \rightarrow \mathbb{R}^{nN}$, where $H(R) \triangleq [F(R_1)^\top, \dots, F(R_N)^\top]^\top$, and $F(R_i)$ denotes the unknown inter-agent interaction dynamics for all $i \in V$.

Assumption 4.1: The function H is less separating than the 2-WL test.

Assumption 4.1 states that the graph-valued function H must not reveal more structural information of G than is able to be distinguished through the 2-WL test. Assumption 4.1 is reasonable since, in practice, any continuous function that at each node aggregates over neighboring nodes and applies a nonlinearity to this aggregated value is provably less separating than the 1-WL test [21]. The 1-WL test is less separating than the 2-WL test, so any function of this form can be universally approximated by a GNN. We refer the reader to [21] for a more complete exposition on the classes of functions that are able to be universally approximated by GNNs.

If (i) the graph-valued function being approximated by the GNN is less separating than the 2-WL test and (ii) the input space of the graph valued function is compact, the universal function approximation property of GNNs in [20, Lemma 3] holds. We note that the function $H(R)$ is an equivariant function of the graph G because the outputs at each node, $F(R_i)$, are a function of each node's features and the features of its one-hop neighborhood. Thus, if the graph G were permuted, $H(R)$ would reflect this permutation.

Let the ensemble vector of the GNN node weights be denoted as $\theta \triangleq [\theta_i^\top]_{i \in V}^\top \in \mathbb{R}^{pN}$. Let the loss function for the GNN Φ be defined as $\mathcal{L}(\theta) \triangleq \int_{\Omega} (\|H(R) - \Phi(R, \theta)\|^2 + \sigma \|\theta\|^2) d\mu(R)$,

where μ denotes the Lebesgue measure, $\sigma \in \mathbb{R}_{>0}$ denotes a regularizing constant, and $\sigma \|\theta\|^2$ represents L_2 regularization. Let $\mathcal{U} \subset \mathbb{R}^{pN}$ denote a user-selected compact, convex parameter search space with a smooth boundary, satisfying $\mathbf{0}_{pN} \in \text{int}(\mathcal{U})$. Additionally, define $\bar{\theta} \in \mathbb{R}$, where $\bar{\theta} \triangleq \max_{\theta \in \mathcal{U}} \|\theta\|$. We denote the ideal parameters of the GNN Φ as $\theta^* \in \mathcal{U} \subset \mathbb{R}^{pN}$ where

$$\theta^* \triangleq \arg \min_{\theta \in \mathcal{U}} \mathcal{L}(\theta). \quad (11)$$

For clarity in the subsequent analysis, we desire the solutions θ^* to (11) to be unique. To this end, the following assumption is made.

Assumption 4.2: [20, Assumption 3] The loss function \mathcal{L} is strictly convex over set \mathcal{U} .

Remark 4.3: The universal function approximation property of GNNs was not invoked in the definition of θ^* . The universal function approximation theorem for GNNs established in [20, Lemma 3] states that the function space of GNNs is dense in $\mathcal{C}_E(\Omega, \mathbb{R}^{nN})$, which denotes the space of real-valued, continuous, equivariant functions that map from Ω to \mathbb{R}^{nN} . Let $\varepsilon : \Omega \rightarrow \mathbb{R}^{nN}$ denote an unknown function representing the reconstruction error that is bounded as $\sup_{G \times R \in \Omega} \|H(R) - \Phi(R, \theta)\| \leq \bar{\varepsilon}$. Therefore, $\int_{\Omega} \|F(R) - \Phi(R, \theta)\|^2 d\mu(R) < \varepsilon^2 \mu(\Omega)$. As a result, for any prescribed $\bar{\varepsilon} \in \mathbb{R}$, there exists a GNN Φ such that for all $i \in V$, there exist weights $\theta_i \in \mathbb{R}^p$ which satisfy $\sup_{G \times R \in \Omega} \|F(R) - \Phi(R, \theta)\| \leq \bar{\varepsilon}$. However, determining a search space \mathcal{U} for an arbitrary ε remains an open challenge. So, we allow \mathcal{U} to be arbitrarily selected in the above analysis, at the expense of guarantees of the approximation accuracy.

The unknown dynamics in (10) are modeled using the GNN Φ at node i as

$$F(R_i) = \phi_i^* + \varepsilon_i(R_i, (R_j)_{j \in \mathcal{N}_i^k}), \quad (12)$$

for all $i \in V$, where θ_i^* are the ideal parameters of the GNN Φ at node i , $\phi_i^* \triangleq \phi_i(R_i, (R_j)_{j \in \mathcal{N}_i^k}, \theta_i^*, (\theta_j^*)_{j \in \mathcal{N}_i^{k-1}})$ and $\varepsilon_i \in \mathbb{R}^n$ denotes the i^{th} component of ε for all $i \in V$, where $\varepsilon \triangleq [\varepsilon_i^\top]_{i \in V}^\top$. The Lb-GNN's approximation of $H(R)$ at node i is given as $\hat{\phi}_i \triangleq \phi_i(R_i, (R_j)_{j \in \mathcal{N}_i^k}, \hat{\theta}_i, (\hat{\theta}_j)_{j \in \mathcal{N}_i^{k-1}})$, where $\hat{\theta}_i \in \mathbb{R}^p$ denotes the Lb-GNN's weight estimates at node i that are subsequently designed through a Lyapunov-based analysis. The approximation objective is to determine optimal estimates of θ such that $R \mapsto \Phi(R, \theta)$ approximates $R \mapsto H(R)$ with minimal error for any $R \in \Omega$.

B. Control Design

Based on (10) and the subsequent stability analysis, the controller at node i is designed as

$$u_i = k_2 \eta_i + \hat{\phi}_i + \sum_{j \in \mathcal{N}_i^{k-1}} \frac{\partial \hat{\phi}_i}{\partial \hat{\theta}_j} (\hat{\theta}_i - \hat{\theta}_j) + (1 - k_1) \dot{x}_d, \quad (13)$$

where $k_2 \in \mathbb{R}_{>0}$ is a user-defined gain, for all $i \in V$. Substituting (12) and (13) into (10) yields

$$\begin{aligned} \dot{\eta}_i &= k_1 \sum_{j \in V \setminus \mathcal{N}_i} g(x_0, y_j) (\eta_j + (1 - k_1) e) \\ &\quad - k_2 \eta_i + \phi_i^* - \hat{\phi}_i + \varepsilon_i - \sum_{j \in \mathcal{N}_i^{k-1}} \frac{\partial \hat{\phi}_i}{\partial \hat{\theta}_j} (\hat{\theta}_i - \hat{\theta}_j). \end{aligned} \quad (14)$$

C. Adaptive Update Law Design

Based on the subsequent stability analysis, we design the distributed adaptive update law for the Lb-GNN as

$$\dot{\hat{\theta}}_i = \text{proj}(\aleph_i), \quad (15)$$

where

$$\aleph_i \triangleq \Gamma_i \left(\left(\sum_{j \in \mathcal{N}_i^{k-1}} \frac{\partial \hat{\phi}_i}{\partial \hat{\theta}_j} \right)^\top \eta_i - k_3 \left(\sum_{j \in \mathcal{N}_i} (\hat{\theta}_i - \hat{\theta}_j) + \hat{\theta}_i \right) \right),$$

where $k_3 \in \mathbb{R}_{>0}$ is a user-defined gain, $\Gamma_i \in \mathbb{R}^{p \times p}$ is a symmetric, positive-definite, user-defined gain matrix, and the projection operator ensures $\hat{\theta} \in \mathcal{U}$ for all $t \in \mathbb{R}_{\geq 0}$, defined as in [24, Appendix E.4]. In the following section, we perform a stability analysis for the ensemble system.

V. STABILITY ANALYSIS

To quantify the approximation given by (12), the parameter estimation error $\tilde{\theta}_i \in \mathbb{R}^p$ at node i is defined as

$$\tilde{\theta}_i \triangleq \theta_i^* - \hat{\theta}_i, \quad (16)$$

for all $i \in V$. Applying a first-order Taylor theorem of ϕ_i^* about the point $(R_i, (R_j)_{j \in \mathcal{N}_i^k}, \hat{\theta}_i, (\hat{\theta}_j)_{j \in \mathcal{N}_i^{k-1}})$ yields

$$\phi_i^* = \hat{\phi}_i + \frac{\partial \hat{\phi}_i}{\partial \hat{\theta}_i} \tilde{\theta}_i + \sum_{j \in \mathcal{N}_i^{k-1}} \frac{\partial \hat{\phi}_i}{\partial \hat{\theta}_j} \tilde{\theta}_j + \sum_{j \in \mathcal{N}_i^{k-1}} T_j, \quad (17)$$

for all $i \in V$, where $T_j \in \mathbb{R}^n$ denotes the first Lagrange remainder, which accounts for the error introduced by truncating the Taylor approximation after the first-order term. Substituting (17) into (14) and using (16) yields

$$\begin{aligned} \dot{\eta}_i &= k_1 \sum_{j \in V \setminus \mathcal{N}_i} g(x_0, y_j) (\eta_j + (1 - k_1) e) \\ &\quad + \varepsilon_i - k_2 \eta_i + \sum_{j \in \mathcal{N}_i^{k-1}} \frac{\partial \hat{\phi}_i}{\partial \hat{\theta}_j} \tilde{\theta}_j + \chi_i, \end{aligned} \quad (18)$$

where $\chi_i \triangleq \sum_{j \in \mathcal{N}_i^{k-1}} \frac{\partial \hat{\phi}_i}{\partial \hat{\theta}_j} (\theta_j^* - \hat{\theta}_j^*) + \sum_{j \in \mathcal{N}_i^{k-1}} T_j$.

Lemma 5.1: [20, Lemma 5] The first Lagrange remainder T_i is upper bounded as $\|T_i\| \leq \rho_{T_1, i}(\|\kappa\|) \|\theta_i\|^2$ for all $i \in V$, where $\rho_{T_1, i} : \mathbb{R}_{\geq 0} \rightarrow \mathbb{R}_{\geq 0}$ is a strictly increasing polynomial that is quadratic in the norm of the ensemble GNN input $\kappa \triangleq [\kappa_i^\top]_{i \in V}^\top \in \mathbb{R}^{Nd^{(in)}}$.

Let $\eta \triangleq [\eta_i^\top]_{i \in V}^\top \in \mathbb{R}^{nN}$ denote the ensemble backstepping error vector for all influencing nodes. Define $\tilde{\theta} \triangleq [\tilde{\theta}_i^\top]_{i \in V}^\top \in \mathbb{R}^{pN}$ and $\Gamma \triangleq \text{blkdiag}\{\Gamma_1, \dots, \Gamma_N\} \in \mathbb{R}^{pN \times pN}$. Define the concatenated state vector as $z \triangleq [e^\top \quad \eta^\top \quad \tilde{\theta}^\top]^\top \in \mathbb{R}^\varphi$, where $\varphi \triangleq n + N(n + p)$. Taking the time derivative of z and substituting (9), (15), and (18) into the resulting expression yields

$$\dot{z} = \begin{bmatrix} h(x_0) - \dot{x}_d + \sum_{i \in V} g(x_0, y_i) (\eta_i + (1 - k_1) e) \\ k_1 \sum_{j \in V \setminus \mathcal{N}_i} g(x_0, y_j) (\eta_j + (1 - k_1) e) + \varepsilon_i \\ -k_2 \eta_i + \sum_{j \in \mathcal{N}_i^{k-1}} \frac{\partial \hat{\phi}_i}{\partial \hat{\theta}_j} \tilde{\theta}_j + \chi_i \\ -[(\text{proj}(\aleph_i))^\top]_{i \in V}^\top \end{bmatrix}_{i \in V}^\top. \quad (19)$$

Consider the candidate Lyapunov function

$$V(z) \triangleq \frac{1}{2} z^\top P z, \quad (20)$$

where $P \triangleq \text{blkdiag}\{I_n, I_{nN}, \Gamma^{-1}\} \in \mathbb{R}^{\varphi \times \varphi}$ and $V : \mathbb{R}^\varphi \rightarrow \mathbb{R}_{\geq 0}$. By the Rayleigh quotient, (20) satisfies

$$\lambda_1 \|z\|^2 \leq V(z) \leq \lambda_2 \|z\|^2, \quad (21)$$

where $\lambda_1 \triangleq \frac{1}{2} \min\{1, \lambda_{\min}(\Gamma^{-1})\}$ and $\lambda_2 \triangleq \frac{1}{2} \max\{1, \lambda_{\max}(\Gamma^{-1})\}$. Based on the subsequent proposition, define $\lambda_3 \in \mathbb{R}_{>0}$ as $\lambda_3 \triangleq \min\{\frac{k_1}{2} \bar{g} N - \bar{g} N - \frac{1}{2} N^3 - \frac{1}{2} N - \frac{\epsilon_1}{2}, \frac{k_2}{4} - k_1 \bar{g} - \frac{1}{2} k_1^2 \bar{g}^2 - \frac{1}{2} \bar{g}^2 - \frac{1}{2} k_1^4 \bar{g}^2, \frac{k_3}{2}\}$.

Proposition 5.2: If the user-defined gains $\epsilon_1 \in \mathbb{R}$, $k_1 \in \mathbb{R}$, $k_2 \in \mathbb{R}$, and $k_3 \in \mathbb{R}$ are sequentially selected to satisfy the sufficient gain conditions $\epsilon_1 > 0$, $k_1 > 2 + \frac{1}{\bar{g} N} (N^3 + N + \epsilon_1)$, $k_2 > 4k_1 \bar{g} + 2\bar{g}^2 (k_1^4 + k_1^2 + 1)$, and $k_3 > 0$, respectively, then $\lambda_3 > 0$.

The universal function approximation property of GNNs only holds over a compact domain; therefore, we require that the inputs to Φ must lie on a compact domain for all $t \in \mathbb{R}_{\geq 0}$. We enforce this condition by proving that $R_i \in \mathcal{Y}_i$, for all $i \in V$. Let $\rho : \mathbb{R}_{\geq 0} \rightarrow \mathbb{R}_{\geq 0}$ denote a strictly increasing function and define $\bar{\rho}(\cdot) \triangleq \rho(\cdot) - \rho(0)$, where $\bar{\rho}$ is strictly increasing and invertible. Consider the compact domain $\mathcal{D} \subset \mathbb{R}^\varphi$, defined as

$$\mathcal{D} \triangleq \left\{ \psi \in \mathbb{R}^\varphi : \|\psi\| \leq \bar{\rho}^{-1}(k_2(\lambda_3 - \lambda_4) - \rho(0)) \right\}, \quad (22)$$

where $\lambda_4 \in \mathbb{R}_{>0}$ is a user-defined rate of convergence. Define the set $\Omega \triangleq G \times \mathcal{Y}$, where $\mathcal{Y} \triangleq \{\psi \in \mathbb{R}^{Nd^{(in)}} : \psi_i \in \mathcal{Y}_i, \forall i \in V\}$, and \mathcal{Y}_i is defined as

$$\begin{aligned} \mathcal{Y}_i &\triangleq \{\psi \in \mathbb{R}^{d^{(in)}} : \|\psi\| \leq (1 + N(k_1 + 1)) \\ &\quad \cdot \bar{\rho}^{-1}(k_2(\lambda_3 - \lambda_4) - \rho(0)) + (1 + N) \bar{x}_d\}, \end{aligned} \quad (23)$$

For the dynamics described by (19), the set of initial conditions $\mathcal{S} \subset \mathcal{D}$ is defined as

$$\mathcal{S} \triangleq \left\{ \psi \in \mathbb{R}^\varphi : \|\psi\| < \sqrt{\frac{\lambda_1}{\lambda_2} \bar{\rho}^{-1}(k_2(\lambda_3 - \lambda_4) - \rho(0)) - \sqrt{\frac{v}{\lambda_4}}} \right\}, \quad (24)$$

and the uniform ultimate bound is defined as

$$\mathcal{U} \triangleq \left\{ \psi \in \mathbb{R}^\varphi : \|\psi\| \leq \sqrt{\frac{\lambda_2 v}{\lambda_1 \lambda_4}} \right\}, \quad (25)$$

where $v \in \mathbb{R}_{>0}$ is defined as $v \triangleq \frac{\bar{\epsilon}^2}{k_2} + \frac{\bar{x}_d^2}{2\bar{g}N} + \frac{\bar{h}^2}{2\epsilon_1} + \frac{1}{2} (2N + 1)^2 k_3 \bar{\theta}^2 N$.

Theorem 5.3: For the influencing nodes' dynamics given by (3) and target node's dynamics given by (4), the controller and adaptive update law in (13) and (15), respectively, guarantee that for any $z(t_0) \in \mathcal{S}$, z exponentially converges to \mathcal{U} in the sense that

$$\|z(t)\| \leq \sqrt{\frac{\lambda_2}{\lambda_1} \left(\frac{v}{\lambda_4} + e^{-\frac{\lambda_4}{\lambda_2}(t-t_0)} \left(\|z(t_0)\|^2 - \frac{v}{\lambda_4} \right) \right)},$$

for all $t \in [t_0, \infty)$, provided that Proposition 5.2 is satisfied, the sufficient gain condition $\lambda_3 > \lambda_4 + \frac{1}{k_2} \rho\left(\sqrt{\frac{\lambda_2 v}{\lambda_1 \lambda_4}}\right)$ is satisfied, and Assumptions 3.1-4.2 hold.

Proof: Taking the time derivative of (20) and substituting (19) into the resulting expression yields

$$\begin{aligned}\dot{V} = & -(k_1 - 1) \sum_{i \in V} g(x_0, y_i) e^\top e + e^\top h(x_0) \\ & - k_2 \eta^\top \eta - e^\top \dot{x}_d + \sum_{i \in V} g(x_0, y_i) e^\top \eta_i \\ & + k_1 \sum_{i \in V} \sum_{j \in V \setminus \bar{\mathcal{N}}_i} g(x_0, y_j) \eta_i^\top \eta_j \\ & + k_1 (1 - k_1) \sum_{i \in V} \sum_{j \in V \setminus \bar{\mathcal{N}}_i} g(x_0, y_j) \eta_i^\top e + \eta^\top \varepsilon \quad (26) \\ & + \sum_{i \in V} \sum_{j \in \bar{\mathcal{N}}_i^{k-1}} \eta_i^\top \frac{\partial \hat{\phi}_i}{\partial \hat{\theta}_j} \tilde{\theta}_j + \eta^\top \chi \\ & - \sum_{i \in V} \tilde{\theta}_i^\top \Gamma_i^{-1} \text{proj}(\mathfrak{N}_i),\end{aligned}$$

where $\chi \triangleq [\chi_i^\top]_{i \in V}^\top \in \mathbb{R}^{nN}$. From [24, Appendix E.4], we have that $\text{proj}(\mathfrak{N}_i) \leq \mathfrak{N}_i$. Using this fact, performing algebraic manipulation, and applying (16) yields

$$\begin{aligned}- \sum_{i \in V} \tilde{\theta}_i^\top \Gamma_i^{-1} \text{proj}(\mathfrak{N}_i) \leq & - \sum_{i \in V} \sum_{j \in \bar{\mathcal{N}}_i^{k-1}} \left(\tilde{\theta}_i^\top \frac{\partial \hat{\phi}_i}{\partial \hat{\theta}_j} \eta_i \right) \\ & + k_3 \sum_{i \in V} \tilde{\theta}_i^\top \tilde{\theta}_i \quad (27) \\ & + k_3 \sum_{i \in V} \sum_{j \in \bar{\mathcal{N}}_i} \tilde{\theta}_i^\top (\tilde{\theta}_j - \tilde{\theta}_i) \\ & + k_3 \sum_{i \in V} \sum_{j \in \bar{\mathcal{N}}_i} \tilde{\theta}_i^\top (\theta_i^* - \theta_j^*).\end{aligned}$$

Using (11), the definition of the graph Laplacian, and expanding $\hat{\theta}_i$ according to (16), (27) is upper bounded as

$$\begin{aligned}- \sum_{i \in V} \tilde{\theta}_i^\top \Gamma_i^{-1} \text{proj}(\mathfrak{N}_i) \leq & - \sum_{i \in V} \sum_{j \in \bar{\mathcal{N}}_i^{k-1}} \left(\tilde{\theta}_i^\top \frac{\partial \hat{\phi}_i}{\partial \hat{\theta}_j} \eta_i \right) \\ & + k_3 \sum_{i \in V} \tilde{\theta}_i^\top \tilde{\theta} - k_3 \tilde{\theta}^\top \tilde{\theta} \quad (28) \\ & + k_3 \sum_{i \in V} \sum_{j \in \bar{\mathcal{N}}_i} \tilde{\theta}_i^\top (\theta_i^* - \theta_j^*).\end{aligned}$$

Using (11), substituting (28) into (26), upper bounding all terms by their norms, and applying the Cauchy-Schwarz inequality yields

$$\begin{aligned}\dot{V} \leq & -(k_1 - 1) \bar{g}N \|e\|^2 - (k_2 - k_1 \bar{g}) \|\eta\|^2 \\ & - k_3 \|\tilde{\theta}\|^2 + \|e\| \bar{x}_d + \bar{g} \sqrt{N} \|\eta\| \|e\| \\ & + k_1 (k_1 + 1) \bar{g}N \sqrt{N} \|\eta\| \|e\| \quad (29) \\ & + \|e\| \bar{h} + \|\eta\| \|\chi\| + \|\eta\| \bar{\varepsilon} \\ & + (2N + 1) k_3 \bar{\theta} \sqrt{N} \|\tilde{\theta}\|.\end{aligned}$$

By Lemma 5.1 and the use of a bounded search space for θ^* in (11), there exist some $\rho_{G_1,j} : \mathbb{R}_{\geq 0} \rightarrow \mathbb{R}_{\geq 0}$ and $\rho_{T_1,j} : \mathbb{R}_{\geq 0} \rightarrow \mathbb{R}_{\geq 0}$ such that $\rho_{G_1,j}$ and $\rho_{T_1,j}$ are strictly increasing functions, where $\|\chi_i\| \leq 2\theta \sum_{j \in \bar{\mathcal{N}}_i^{k-1}} \rho_{G_1,j}(\|R\|) + \sum_{j \in \bar{\mathcal{N}}_i^{k-1}} \rho_{T_1,j}(\|R\|) \|\tilde{\theta}_j\|^2$, for all $i \in V$. From (11) and the definition of R , there exist some $\rho_{1,i} : \mathbb{R}_{\geq 0} \rightarrow \mathbb{R}_{\geq 0}$ where $\rho_{1,i}$

are strictly increasing functions such that $\|\chi_i\| \leq \rho_{1,i}(\|z\|) \|z\|$, for all $i \in V$. Using the Cauchy-Schwarz inequality, it follows that $\|\eta\| \|\chi\| \leq \|\eta\| \rho_2(\|z\|) \|z\|$, where $\rho_2 : \mathbb{R}_{\geq 0} \rightarrow \mathbb{R}_{\geq 0}$ is a strictly increasing function. By completing the square, we upper bound $\|\eta\| \|\chi\|$ as

$$\|\eta\| \|\chi\| \leq \frac{1}{k_2} \rho(\|z\|) \|z\|^2 + \frac{k_2}{2} \|\eta\|^2, \quad (30)$$

where $\rho : \mathbb{R}_{\geq 0} \rightarrow \mathbb{R}_{\geq 0}$ is a strictly increasing function that satisfies $\frac{1}{2} \rho_2^2(\|z\|) \leq \rho(\|z\|)$. Substituting (30) into (29), applying Assumptions 3.1 and 3.2, and applying Young's inequality yields

$$\begin{aligned}\dot{V} \leq & - \left(k_1 \bar{g}N - \bar{g}N - \frac{1}{2} N^3 - \frac{1}{2} N \right) \|e\|^2 \\ & - \left(\frac{k_2}{2} - k_1 \bar{g} - \frac{1}{2} k_1^2 \bar{g}^2 - \frac{1}{2} \bar{g}^2 - \frac{1}{2} k_1^4 \bar{g}^2 \right) \|\eta\|^2 \quad (31) \\ & - k_3 \|\tilde{\theta}\|^2 + \frac{1}{k_2} \rho(\|z\|) \|z\|^2 + \|e\| \bar{x}_d \\ & + \|\eta\| \bar{\varepsilon} + (2N + 1) k_3 \bar{\theta} \sqrt{N} \|\tilde{\theta}\| + \|e\| \bar{h}.\end{aligned}$$

Completing the square and applying the triangle inequality to (31) yields

$$\begin{aligned}\dot{V} \leq & - \left(\frac{k_1}{2} \bar{g}N - \bar{g}N - \frac{1}{2} N^3 - \frac{1}{2} N - \frac{\epsilon_1}{2} \right) \|e\|^2 \\ & - \left(\frac{k_2}{4} - k_1 \bar{g} - \frac{1}{2} k_1^2 \bar{g}^2 - \frac{1}{2} \bar{g}^2 - \frac{1}{2} k_1^4 \bar{g}^2 \right) \|\eta\|^2 \quad (32) \\ & - \frac{k_3}{2} \|\tilde{\theta}\|^2 + \left(\frac{\bar{\varepsilon}^2}{k_2} + \frac{\bar{h}^2}{2\epsilon_1} + \frac{\bar{x}_d^2}{2\bar{g}N} \right. \\ & \left. + \frac{1}{2} (2N + 1)^2 k_3 \bar{\theta}^2 N \right) + \frac{1}{k_2} \rho(\|z\|) \|z\|^2.\end{aligned}$$

Substituting the definitions of λ_3 and v into (32) gives

$$\dot{V} \leq - \left(\lambda_3 - \frac{1}{k_2} \rho(\|z\|) \right) \|z\|^2 + v, \quad (33)$$

for all $t \in \mathcal{I}$. Since the solution $t \mapsto z(t)$ is continuous, there exists a time interval $\mathcal{I} \triangleq [t_0, t_1]$ with $t_1 > t_0$ such that $z \in \mathcal{D}$ for all $t \in \mathcal{I}$. Since $z(t_0) \in \mathcal{S}$ and ρ is a strictly increasing function, (33) can be written as

$$\dot{V} \leq - \frac{\lambda_4}{\lambda_2} V(z) + v, \quad (34)$$

for all $t \in \mathcal{I}$. Solving the differential inequality in (34) over \mathcal{I} yields

$$V(z(t)) \leq V(z(t_0)) e^{-\frac{\lambda_4}{\lambda_2}(t-t_0)} + \frac{\lambda_2 v}{\lambda_4} \left(1 - e^{-\frac{\lambda_4}{\lambda_2}(t-t_0)} \right). \quad (35)$$

Applying (21) to (35) yields

$$\|z(t)\| \leq \sqrt{e^{-\frac{\lambda_4}{\lambda_2}(t-t_0)} \left(\frac{\lambda_2}{\lambda_1} \|z(t_0)\|^2 - \frac{\lambda_2 v}{\lambda_1 \lambda_4} \right) + \frac{\lambda_2 v}{\lambda_1 \lambda_4}}, \quad (36)$$

for all $t \in \mathcal{I}$. Next, we must show that \mathcal{I} can be extended to $[t_0, \infty)$. Let $t \mapsto z(t)$ be a solution to the ordinary differential equation in (19) with initial condition $z(t_0) \in \mathcal{S}$, as defined in (24). By [24, Lemma E.1], the projection operator is locally Lipschitz in its arguments. Then, the right hand side of (19) is

piecewise continuous in t and locally Lipschitz in z for $t \geq t_0$ where $z \in \mathbb{R}^\varphi$. By (36), it follows that

$$\|z(t)\| < \sqrt{\frac{\lambda_1}{\lambda_2}} \|z(t_0)\| + \sqrt{\frac{\lambda_2 v}{\lambda_1 \lambda_4}}, \quad (37)$$

for all $t \in \mathcal{I}$. Since $z(t_0) \in \mathcal{S}$ for all $t \in \mathcal{I}$, we have

$$\|z(t_0)\| < \sqrt{\frac{\lambda_1}{\lambda_2}} \bar{\rho}^{-1} (k_2 (\lambda_3 - \lambda_4) - \rho(0)) + \sqrt{\frac{v}{\lambda_4}}. \quad (38)$$

Applying (38) to (37) gives $\|z(t_0)\| \leq \bar{\rho}^{-1} (k_2 (\lambda_3 - \lambda_4) - \rho(0))$ for all $t \in \mathcal{I}$, which by the definition of (22), yields $z(t) \in \mathcal{D}$ for all $t \in \mathcal{I}$. Since $z(t)$ remains in the compact set $\mathcal{D} \subset \mathbb{R}^\varphi$ for all $t \in \mathcal{I}$, a unique solution $z(t)$ exists for all $t \geq t_0$ [25, Theorem 3.3]. Therefore, $\mathcal{I} = [t_0, \infty)$. Thus, for $z(t_0) \in \mathcal{S}$, (36) holds for all $z(t) \in \mathcal{D}$ for all $t \in \mathcal{I}$. The limit of (36) as $t \rightarrow \infty$ yields $\|z\| \leq \sqrt{\frac{\lambda_2 v}{\lambda_1 \lambda_4}}$, which indicates that $z(t)$ converges to the set \mathcal{U} , as defined in (25).

We must prove that $R_i \in \mathcal{Y}_i$ for all $i \in V$. Using (5), Assumption 3.2, and the triangle inequality yields $\|x_0\| \leq \bar{x}_d + \|e\|$. Similarly, using (6), (8), and the triangle inequality yields $\|y_i\| \leq k_1 \|e\| + \bar{x}_d + \|\eta\|$, for all $i \in V$. By the definitions of Q_i and z , it follows that

$$\|R_i\| \leq (1 + N(k_1 + 1)) \|z\| + (1 + N) \bar{x}_d, \quad (39)$$

for all $i \in V$. Therefore, $G \times R \in \Omega$ for all $t \in \mathcal{I}$ and the universal function approximation property of GNNs described in [20, Lemma 3] holds for all $t \in \mathcal{I}$.

Since $z \in \mathcal{D}$ for all $t \in [t_0, \infty)$ it follows that from (23) and (39) that $R_i \in \mathcal{Y}_i$ for all $i \in V$. Therefore, $z \in \mathcal{D}$ implies $G \times R \in \Omega$, and the universal function approximation property for GNNs holds everywhere.

Since $\|z\| \leq \bar{\rho}^{-1} (k_2 (\lambda_3 - \lambda_4) - \rho(0))$, $\|e\|$, $\|\eta\|$, $\|\tilde{\theta}\|$ are bounded. Therefore, $e, \eta, \theta \in \mathcal{L}_\infty$. By Assumption 3.2, $x_d \in \mathcal{L}_\infty$ and since $e, \eta \in \mathcal{L}_\infty$, then $R \in \mathcal{L}_\infty$. Based on the fact that $\tilde{\theta} \in \mathcal{L}_\infty$, the use of the projection operator in (15), and the use of a bounded search space in (11), we have $\hat{\theta} \in \mathcal{L}_\infty$ where $\hat{\theta} \triangleq [\hat{\theta}_i^\top]_{i \in V}^\top \in \mathbb{R}^{pN}$. Let $\hat{\Phi} \triangleq [\hat{\phi}_i^\top]^\top \in \mathbb{R}^{nN}$. Based on the use of activation functions with bounded derivatives and the fact that $R, \hat{\theta} \in \mathcal{L}_\infty$, the norm of the derivative of the GNN $\hat{\Phi}$ with respect to the weight estimates and the norm of the GNN $\hat{\Phi}$ are bounded. Let $u \triangleq [u_i^\top]_{i \in V}^\top \in \mathbb{R}^{nN}$. By Assumption 3.2 and since $\eta, \hat{\theta} \in \mathcal{L}_\infty$, the norm of derivative of the GNN $\hat{\Phi}$ with respect to the weight estimates is bounded, and the norm of the GNN $\hat{\Phi}$ is bounded, $u \in \mathcal{L}_\infty$. Since $\eta, \hat{\theta} \in \mathcal{L}_\infty$ and that the norm of derivative of the GNN $\hat{\Phi}$ with respect to the weight estimates is bounded, $\hat{\theta} \in \mathcal{L}_\infty$. ■

VI. SIMULATION

Using the control law in (13) and the adaptive weight update law in (15), a simulation is performed where a network of $N = 4$ nodes with a fully connected communication graph indirectly influences a target node to follow a desired trajectory, given by

$$x_d = \begin{bmatrix} 10 \sin(0.01t) \\ 10 \sin(0.025t) \cos(0.025t) \\ 5 \sin(0.075t) \end{bmatrix} m.$$

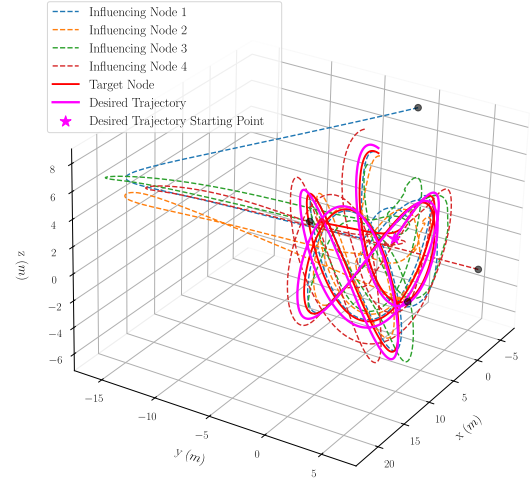


Fig. 1. Visualization of the trajectories of the target node and the influencing nodes for $t \in [0, 360]$ s.

The target node's interaction dynamics were selected as $g(x_0, y_i) = 0.1 \exp(-\frac{1}{1,000,000} (x_0 - y_i)^\top (x_0 - y_i)) s^{-1}$. [4]. The inter-agent interaction dynamics were selected as $f(Q_i) = 50 \sum_{j \in \mathcal{N}_i} \frac{y_i - y_j}{\|y_i - y_j\|^3} m/s$ [3]. The target drift dynamics were selected such that $h(x_0) = [-0.057 \cos(x_{0,1}), 0.03 \sin(x_{0,2}), -0.008 \cos(x_{0,3})]^\top m/s$. These dynamics enable a repulsive effect between nodes. The initial positions of the influencing nodes were selected as $y_1(t_0) = [-6 \ -1 \ 8]^\top m$, $y_2(t_0) = [6 \ 4 \ -2]^\top m$, $y_3(t_0) = [4 \ -6 \ 1]^\top m$, and $y_4(t_0) = [-4, 6, -2]^\top m$. The target node is initialized at $x_0(t_0) = [6 \ -4 \ 2]^\top m$. For all $j \in \{0, \dots, k\}$, the Lb-GNN weight estimates were initialized with random values drawn from a uniform distribution $W_i^{(j)} \sim U(0, 0.3)$, for all $i \in V$. The size of the parameter search space was selected as $\bar{\theta} = 10$. Due to the message-passing framework of the GNN, the number of required successive communications between neighbors is equivalent to the number of message-passing layers in the network. In the multi-agent control literature, the number of GNN layers is typically limited to between 1 and 4 layers[17], [18]. The Lb-GNN Φ has two hidden layers ($k = 2$) and eight neurons per hidden layer, for all $i \in V$. The swish activation function was used for all hidden layers, and $\tanh(\cdot)$ was used on the output layer. For all $i \in V$, the gain values were empirically selected as $k_1 = 3.5$, $k_2 = 12$, $k_3 = 0.001$, and $\Gamma_i = 2 \cdot I_{p \times p}$. The simulation was run for 360 seconds. A three-dimensional visualization of the trajectories of the influencing and target nodes is presented in Figure 1.

The simulation resulted in an RMS position tracking error of $\|e\|_{\text{RMS}} = 0.61 m$, a mean RMS control effort of $\|u\|_{\text{RMS}} = 19.57 m/s$, and a mean RMS function approximation error of $\|\tilde{\Phi}\|_{\text{RMS}} = 15.95 m/s$, where $\tilde{\Phi} \triangleq \Phi(R, \theta) - H(R)$ denotes the function approximation error for the GNN Φ .

Figure 2 shows the ability of the designed control law to allow multiple nodes to influence a target node to within a neighborhood of a desired trajectory. As seen in Figure 2, the

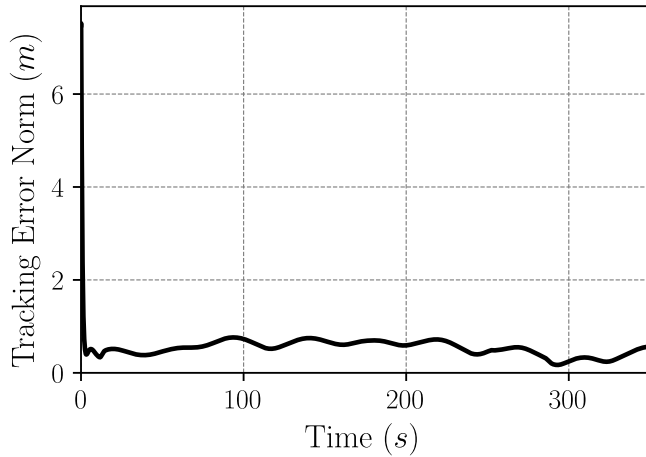


Fig. 2. Visualization of the position tracking error of the target node for $t \in [0, 360]$ s.

norm of the tracking error converges to within an ultimate bound of approximately 1 m after 5 seconds.

VII. CONCLUSION

In this work, we developed the first Lb-GNN-based control law for the indirect influence problem. Our method enables a team of cooperative nodes to regulate a target node to within a neighborhood of a desired trajectory despite uncertain inter-agent interaction dynamics. Numerical simulations validate the theoretical findings. Future work will examine influence strategies with formation control in the presence of multiple targets.

REFERENCES

- [1] A. J. King, S. J. Portugal, D. Strömbom, R. P. Mann, J. A. Carrillo, D. Kalise, G. de Croon, H. Barnett, P. Scerri, R. Groß, D. R. Chadwick, and M. Papadopoulou, "Biologically inspired herding of animal groups by robots," *Methods Ecol. Evol.*, vol. 14, no. 2, pp. 478–486, 2023.
- [2] A. Bazzan and F. Klugl, *Multi-Agent Systems for Traffic and Transportation Engineering*. IGI Global, 2009.
- [3] E. Sebastián, E. Montijano, and C. Sagüés, "Adaptive multirobot implicit control of heterogeneous herds," *IEEE Trans. Robot.*, vol. 38, no. 6, pp. 3622–3635, 2022.
- [4] R. Licitra, Z. Bell, and W. Dixon, "Single agent indirect herding of multiple targets with unknown dynamics," *IEEE Trans. Robot.*, vol. 35, no. 4, pp. 847–860, 2019.
- [5] Y. Cao and W. Ren, "Containment control with multiple stationary or dynamic leaders under a directed interaction graph," in *Proc. IEEE Conf. Decis. Control*, 2009, pp. 3014–3019.
- [6] M. H. Stone, "The generalized Weierstrass approximation theorem," *Math. Mag.*, vol. 21, no. 4, pp. 167–184, 1948.
- [7] K. Hornik, "Approximation capabilities of multilayer feedforward networks," *Neural Netw.*, vol. 4, pp. 251–257, 1991.
- [8] P. Kidger and T. Lyons, "Universal approximation with deep narrow networks," in *Conf. Learn. Theory*, 2020, pp. 2306–2327.
- [9] I. Goodfellow, Y. Bengio, and A. Courville, *Deep Learning*. MIT Press, 2016, vol. 1.
- [10] D. Rolnick and M. Tegmark, "The power of deeper networks for expressing natural functions," in *Int. Conf. Learn. Represent.*, 2018.
- [11] Y. LeCun, Y. Bengio, and G. Hinton, "Deep learning," *Nature*, vol. 521, no. 7553, pp. 436–444, 2015.
- [12] C. F. Nino, O. S. Patil, J. Philor, Z. Bell, and W. E. Dixon, "Deep adaptive indirect herding of multiple target agents with unknown interaction dynamics," in *Proc. IEEE Conf. Decis. Control*, 2023, pp. 2509–2514.
- [13] C. F. Nino, O. S. Patil, S. C. Edwards, Z. I. Bell, and W. E. Dixon, "Distributed target tracking under partial feedback using Lyapunov-based deep neural networks," in *Proc. IEEE Conf. Decis. Control*, 2024, pp. 5274–5279.
- [14] W. Makumi, Z. Bell, J. Philor, and W. E. Dixon, "Cooperative approximate optimal indirect regulation of uncooperative agents with Lyapunov-based deep neural network," in *AIAA SciTech*, 2024.
- [15] J. Philor, W. Makumi, Z. Bell, and W. E. Dixon, "Approximate optimal indirect control of an unknown agent within a dynamic environment using a Lyapunov-based deep neural network," in *Proc. Am. Control Conf.*, 2024, pp. 3430–3435.
- [16] X. Ji, H. Li, Z. Pan, X. Gao, and C. Tu, "Decentralized, unlabeled multi-agent navigation in obstacle-rich environments using graph neural networks," in *IEEE Conf. Intell. Robot. Syst. (IROS)*, 2021, pp. 8936–8943.
- [17] F. Gama, E. Tolstaya, and A. Ribeiro, "Graph neural networks for decentralized controllers," in *Proc. IEEE Int. Conf. Acoustics, Speech, and Signal Processing (ICASSP)*, 2021, pp. 5260–5264.
- [18] Q. Li, F. Gama, A. Ribeiro, and A. Prorok, "Graph neural networks for decentralized multi-robot path planning," in *Proc. IEEE Int. Conf. Conf. Intell. Robot. Syst. (IROS)*, 2020, pp. 11 785–11 792.
- [19] A. Sanchez-Gonzalez, N. Heess, J. T. Springenberg, J. Merel, M. Riedmiller, R. Hadsell, and P. Battaglia, "Graph networks as learnable physics engines for inference and control," in *Proc. 35th Conf. Mach. Learn.*, 2018, pp. 4470–4479.
- [20] B. C. Fallin, C. F. Nino, O. S. Patil, Z. I. Bell, and W. E. Dixon, "Lyapunov-based graph neural networks for adaptive control of multi-agent systems," *arXiv preprint arXiv:2503.15360*, 2025.
- [21] W. Azizian and M. Lelarge, "Expressive power of invariant and equivariant graph neural networks," *Proc. Int. Conf. Learn. Represent.*, 2020.
- [22] W. L. Hamilton, *Graph Representation Learning*. Morgan & Claypool Publishers, 2020.
- [23] D. Le, X. Luo, L. Bridgeman, M. Zavlanos, and W. E. Dixon, "Single-agent indirect herding of multiple targets using metric temporal logic switching," in *Proc. IEEE Conf. Decis. Control*, 2020, pp. 1398–1403.
- [24] M. Krstic, I. Kanellakopoulos, and P. V. Kokotovic, *Nonlinear and Adaptive Control Design*. New York: John Wiley & Sons, 1995.
- [25] H. K. Khalil, *Nonlinear Systems*, 3rd ed. Prentice Hall, 2002.